
Since January 2020 Elsevier has created a COVID-19 resource centre with free information in English and Mandarin on the novel coronavirus COVID-19. The COVID-19 resource centre is hosted on Elsevier Connect, the company's public news and information website.

Virology 528 (2019) 176–180

Contents lists available at ScienceDirect

Virology

journal homepage: www.elsevier.com/locate/virology

# Identification and formation mechanism of a novel noncoding RNA produced by avian infectious bronchitis virus

Hongliu An[a], Zhichao Cai[a], Yuying Yang[b], Zhaoxiong Wang[b], Ding Xiang Liu[c,*], Shouguo Fang[a,b,**]

[a] College of Agriculture, Yangtze University, 88 Jingmilu, Jingzhou 434025, Hubei, PR China
[b] College of Animal Sciences, Yangtze University, 88 Jingmilu, Jingzhou 434025, Hubei, PR China
[c] South China Agricultural University, Guangdong Province Key Laboratory Microbial Signals & Disease Co, and Integrative Microbiology Research Centre, Guangzhou 510642, Guangdong, PR China

A B S T R A C T

Viral noncoding (nc) RNAs have been shown to play important roles in viral life cycle. Many viruses employ different mechanism to produce ncRNAs. Here, we report that coronavirus infectious bronchitis virus (IBV) produces a novel ncRNA in virus-infected cells. This ncRNA consists of 563 nucleotides excluding a poly(A) tail, is mainly derived from the 3′-untranslated region of IBV genome, and contains a 63-nt-long of terminal leader sequence derived from the 5′ end of the viral genome. Using mutagenesis and reverse genetics, we reveal that this ncRNA is a subgenomic RNA generated by discontinuous transcription mechanism.

## 1. Introduction

Viruses employ different mechanisms to produce a number of noncoding (nc) RNAs excluding microRNA. These ncRNAs mainly include: (1) Viral ncRNAs transcribed by RNA polymerase (Pol) III. For example, two virus-associated (VA) RNAs encoded by Human adenovirus (Reich et al., 1966; Steitz et al., 2010), EBER1 and EBER2 encoded by Epstein–Barr virus (Skalsky and Cullen, 2015), miRNA precursors encoded by murine γ-herpesviral tRNA-pre-miRNA chimeras (Bogerd et al., 2010; Bowden et al., 1997; Diebel et al., 2010) and retrovirus (Kincaid et al., 2012), and intragenic viral small ncRNA encoded by Human bocavirus 1 (Wang et al., 2017); (2) Viral ncRNAs transcribed by RNA polymerase II. For example, polyadenylated nuclear (PAN) RNA encoded by Kaposi's sarcoma-associated herpesvirus (Sun et al., 1996; Zhong and Ganem, 1997), the ~2-kb latency-associated transcript (LAT) expressed by Herpes simplex virus (Bloom, 2004), a conserved ~5-kb intron expressed by Human cytomegalovirus (hCMV) (Kulesza and Shenk, 2004), and a 7.2-kb RNA expressed by mouse CMV (Kulesza and Shenk, 2006), U-rich RNAs (HSURs) produced by Herpesvirus saimiri (HVS), (Albrecht and Fleckenstein, 1992; Ensser and Fleckenstein, 2005); (3) Subgenomic ncRNAs from single-stranded RNA viruses by incomplete degradation of genomic RNA by the cellular 5–3′ exonuclease XRN1. For example, subgenomic RNA (sfRNA) produced by Flaviviruses, such as Dengue virus (DENV), West Nile virus (WNV), Yellow fever virus (YFV), and Zika virus [reviewed in (Bidet and Garcia-Blanco, 2014; Roby et al., 2014; Pijlman et al., 2008; Akiyama et al., 2016), and subgenomic ncRNA generated by some plant viruses such as Barley yellow dwarf virus and Red clover necrotic mosaic virus using similar mechanism (Miller et al., 2016a).

Viral ncRNAs play important roles in viral life cycle. Adenovirus VA RNAs are characterized for their role in counteracting the host antiviral defense through inhibition of protein kinase R (PKR) (Mathews and Shenk, 1991; Wilson et al., 2014). EBER2 regulates the expression of a subset of EBV latent genes throung the interaction of EBER2 and a cellular transcription factor paired box protein 5 (PAX5) (Arvey et al., 2012; Lee et al., 2015). Degradation of miR-27 by mediated HSUR 1 promotes activation and presumably proliferation of HVS-infected host T cells (Cazalla et al., 2010; Guo et al., 2014). KSHV PAN RNA is essential for virion production (Borah et al., 2011).β-herpesvirus HCMV-encoded β2.7 prevents mitochondria-induced apoptosis, enabling steady ATP production for viral processes and persistent infection (Campbell et al., 2008; Stern-Ginossar et al., 2012). SfRNA produced by Flaviviruses is required for cytopathicity and pathogenicity (Pijlman et al., 2008). It has been demonstrated to 1) interfere with cellular RNA decay pathways by inhibiting XRN1 (Moon et al., 2012), 2) dampen the antiviral activity of type I interferon (Schuessler et al., 2012) and 3) inhibit the RNAi pathway in both the vertebrate and arthropod hosts, most likely by serving as a decoy substrate for Dicer (Schnettler et al., 2012). Inhibition of the host interferon response appears to be, at least in some Flaviviruses, achieved by binding and inactivating cellular

* Corresponding author.
** Corresponding author at: College of Agriculture, Yangtze University, 88 Jingmilu, Jingzhou 434025, Hubei, PR China.
*E-mail addresses:* dxliu0001@163.com (D.X. Liu), sg-fang@hotmail.com (S. Fang).

https://doi.org/10.1016/j.virol.2018.12.019
Received 28 September 2018; Received in revised form 19 December 2018; Accepted 26 December 2018
Available online 05 January 2019
0042-6822/ 

regulators of translation of interferon-upregulated mRNAs (Bidet et al., 2014). NcRNAs encoded by some plant RNA viruses can inhibit host translation and overwhelm host's RNA interference system to favor virus infection (Miller et al., 2016b).

Avian infectious bronchitis virus (IBV) belongs to the genus Gammacoronavirus within the order Nidovirales. IBV is an enveloped positive-sense, single-stranded RNA virus causing the acute highly contagious poultry disease infectious bronchitis (Cavanagh, 2005). Like other coronaviruses, IBV can produce sgRNAs via a discontinuous transcription mechanism to encode its structural proteins and specific accessory proteins (Masters, 2006; Sawicki et al., 2007). Briefly, IBV produces six mRNA species in the infected cells, including its genomic mRNA1, sgRNA2 encoding spike (S) protein, sgRNA3 encoding 3a, 3b and envelope (E) protein, sgRNA4 encoding membrane (M) protein, sgRNA5 encoding 5a and 5b, and sgRNA6 encoding nucleocapsid (N) protein. Recently, a low-abundance sgRNA located between the sgRNA4 and 5 has been identified (Bentley et al., 2013).

In this study, we identify firstly an ncRNA in the IBV-infected cells. Moreover, we prove that this ncRNA is derived mainly from 3′ UTR of viral genome and is generated by discontinuous transcription process.

## 2. Materials and methods

### 2.1. Cells and viruses

Vero and chicken embryo fibroblast DF1 cells were maintained in Dulbecco's modified Eagle's medium (DMEM) supplemented with 10% fetal bovine serum (FBS), penicillin (100 units/ml) and streptomycin (100 units/ml) (Invitrogen). A recombinant IBV (rIBV) (Fang et al., 2007) generated from an infectious clone reference genome (IBV Beaudette P65, GenBank accession number DQ001339.1) was used as the wild-type control. All IBV mutants were propagated in Vero cells in FBS-free DMEM. Virus stocks were made through three repeated freeze-thaw cycles and kept at −80 °C in 0.5–1 ml aliquots until use.

### 2.2. Generation of mutant viruses

Constructs containing mutation or deletion were produced by using a QuikChange site-directed mutagenesis kit (Stratagene). The full-length cDNA was assembled as previously described (Fang et al., 2007) by replacing the corresponding fragment with the mutant fragment. The mutations were verified by automated nucleotide sequencing. Full-length transcripts were generated in vitro using the mMessage mMachine T7 kit (Ambion, Austin, TX) according to the manufacturer's instructions, and electroporated into Vero cells with one pulse at 450 V and 50 μF with a Bio-Rad Gene Pulser II electroporator. The transfected Vero cells were cultured overnight in 1% FBS-containing DMEM and further cultured in DMEM without FBS. The transfected cells were monitored daily for formation of cytopathic effect (CPE). Recovered viruses were plaque purified and passaged on Vero cells.

### 2.3. Plague assay and virus titration

Vero cells in 6-well plates were infected with a dilution series of viruses for 1 h, washed twice with medium. Cells were overlaid with 0.4% agar in FBS-free DMEM, incubated at 37 °C for 3–4 days, fixed with 10% formaldehyde, and stained with 0.2% crystal violet. The number of plaques was counted and the virus titer was calculated as plaque-forming unit (PFU) per ml.

### 2.4. Infection of chicken embryos

Ten-day-old embryonated, pathogen-free chicken eggs were inoculated with IBV as described previously (Shen et al., 2009). The allantoic fluid and different organs were harvested after the embryos were chilled at 4 °C overnight. Total RNA was extracted from the homogenized tissues and used for RT-PCR analysis.

### 2.5. RT-PCR analysis

Total RNA was isolated from IBV-infected cells using TRIzol Reagent® (Invitrogen) according to the manufacturer's instructions. The concentration of the total RNA extracted was quantified using a NanoDrop™ 1000 Spectrophotometer (NanoDrop Technologies, Inc., Thermo Fisher Scientific, USA). Reverse transcription (RT) was performed with oligo(dT)18 or specific primer using reverse transcriptase (Promega) according to the manufacturer's instructions. For the detection of viral positive-stranded subgenomic (sg)RNA, oligo(dT)18 was used for cDNA synthesis; for negative-stranded sgRNA, IBV-5′end-F (5′-$_{1}$ACTTAAGATAGATATTAATATATA) was used. IBV-5′end-F and IBV-3′end-R (5′-$_{27608}$TGCTCTAACTCTATACTAGC) were used for PCR.

### 2.6. Western blotting

IBV-infected cells at different time point post-infection were washed with PBS and lysed with 2 × SDS loading buffer containing 100 mM dithiothreitol (DTT), boiled at 100 °C for 5 min, and clarified. The proteins were separated by SDS-PAGE and transferred to a polyvinylidene difluoride (PVDF) membrane (Stratagene). The membrane was blocked overnight at 4 °C or for 2 h at room temperature in blocking buffer (5% fat-free milk powder in phosphate-buffered saline (PBS) buffer containing 0.1% Tween 20 (PBST)) and then was incubated with diluted primary antibodies in blocking buffer for 2 h at room temperature. After the membrane was washed three times with PBST, it was incubated with 1:2000 diluted anti-mouse or anti-rabbit IgG antibodies conjugated with horseradish peroxidase (Dako) in blocking buffer for 1 h at room temperature. After the membrane was washed three times with PBST, the polypeptides were detected with a chemiluminescence detection kit (ECL kit; Amersham Biosciences) according to the manufacturer's instructions. The films were exposed and developed.

### 2.7. Quantitative real-time PCR

Quantitative real-time PCR (qPCR) was used to validate gene expression changes in infected cells. Total RNA (2 μg) was reversedly transcribed to cDNA, and the resulting cDNA was subjected to qPCR using Power SYBR Green PCR Master Mix (Applied Biosystems). Amplification and data collection were performed as manufacturer's instruction (Applied Biosystems 7500 real-time PCR system). The relative gene expression levels were measured using GAPDH as an internal reference, and normalized to gene expression in mock-infected cells (relative expression = 1). All experiments were performed in triplicate.

## 3. Results

### 3.1. Identification of a novel small sgRNA in the IBV-infected cells

In the virus–infected cells, IBV produces six mRNA species, including the genome-length mRNA1 and five subgenomic mRNAs via a discontinuous transcription mechanism. This mechanism is mediated by transcription-regulating sequences (TRSs) in the 3′ end of the leader (TRS-L) and the preceding each mRNA body (TRS-B). TRSs comprise a conserved core sequence (CS) [CU(U/G)AACAA] in IBV. Each mRNA possesses a leader sequence of 64 nucleotides derived from the 5′-end of the genome. In general, six mRNAs are readily detected by Northern blotting in the infected cells.

When probing the viral positive- or negative-stranded mRNA6 by RT-PCR, an unexpected PCR product was concurrently amplified in the IBV-infected Vero cells as well as in chicken embryos (Fig. 1). It is smaller than mRNA6. Subsequently, this product was cloned and

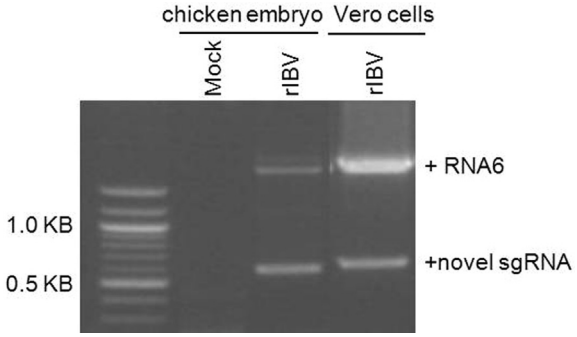


**Fig. 1.** Detection of a novel sgRNA in virus-infected Vero cells and chicken embryo by RT-PCR. Total RNA was extracted from the rIBV-infected Vero cells and chicken embryo. cDNA was synthesized by reverse transcription using oligo (dT)18 as a primer. PCR was performed using primers IBV-5′end-F and IBV-3′end-R. The amplicons were analyzed on 1% agarose gel electrophoresis.

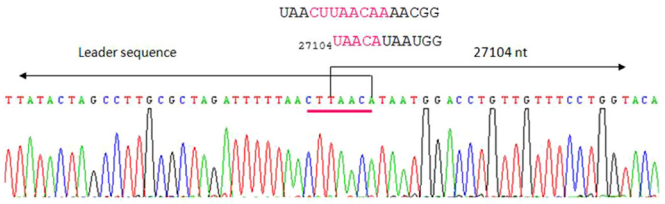


**Fig. 2.** Sequence of the junction between IBV 3′-UTR and the leader at 5′-end of viral genome, indicating the formation of a novel sgRNA mediated by $_{27104}$UAACA$_{27108}$. Vero cells were infected with rIBV at an MOI of 1 PFU/cell. Total RNA extracted from the infected cells was used for reverse transcription using primer oligo(dT)18. PCR was carried out using primers IBV-5′end-F and IBV-3′end-R. PCR product was cloned and sequenced.

sequenced. Sequence analysis indicated that it consists of 563 nucleotides excluding a poly(A) tail, is mainly derived from the 3′-UTR (from nucleotides 27104–27608) of IBV genome, and contains a 63-nt-long of terminal leader sequence derived from the 5′ end of the viral genome (Fig. 2). The results showed the generation of a novel sgRNA in the IBV-infected cells. This sgRNA may be overlooked in previous studies because of its smaller size and lower level of transcription. Due to lack of start codon AUG, this sgRNA is designated as a noncoding RNA (ncRNA). Insertion of an ORF encoding EGFP (carrying its own start codon) between 27149 and 27150 nt of IBV 3′-UTR allowed the

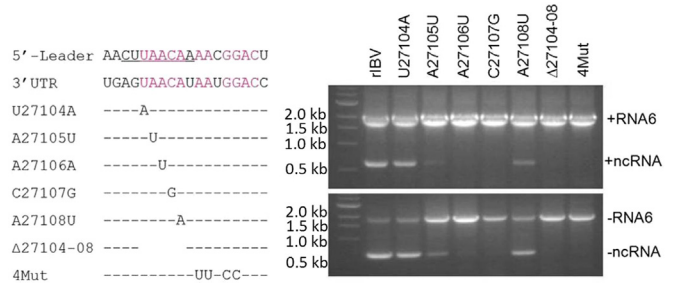


**Fig. 4.** Effect of single nucleotide in the motif UAACA and downstream nucleotides on the generation of ncRNA. Recombinant IBVs containing different mutation(s) and deletion were recovered by reverse genetics (shown in the left panel). Vero cells were infected with rIBV and mutant viruses at an MOI of 1 PFU/cell. Total RNA extracted from the infected cells at 12 h post-infection was used for RT-PCR. The effect of mutation and deletion on the generation of ncRNA was evaluated by detecting the negative- and positive-strand ncRNA synthesis in the cells infected with rIBV and mutant viruses (right panel).

recovery of recombinant virus. RT-PCR analysis showed the presence of the EGFP-containing sgRNA and fluorescence confirmed EGFP expression in virus-infected cells (Fig. 3), implying that the ncRNA is an mRNA. However, this virus was unstable and a deletion of 377 nucleotide acids (from 81 to 457 nt) of EGEP sequences was detected in passage 3 in Vero cells (data not shown).

### 3.2. ncRNA is generated by discontinuous transcription

Further sequence comparison revealed that a sequence motif (UAACA), located in the junction between the 5′ end leader sequence and the 3′-UTR of ncRNA, is shared by 5′-terminus of 3′-UTR and the core sequence (CUUAACAA) within IBV TRS (Fig. 2). These results prompt us to speculate that this ncRNA, like the other viral sgRNA, may be generated by a discontinuous transcription mechanism via template switch mediated by a noncanonical core sequence (UAACA). To confirm this hypothesis, we analyzed the effect of several mutations on ncRNA generation by mutagenesis and reverse genetics. As shown in Fig. 4, compared to wild-type rIBV, single mutation U27104A and A27108U had no or minor effect on ncRNA synthesis; A27105U resulted in a significant reduction in the ncRNA generation, while mutation C27107G, A27106U and deletion of five nucleotides (Δ27104-08) completely abolished the synthesis of both positive-stranded and negative-stranded ncRNA (Fig. 4), suggesting that at least three

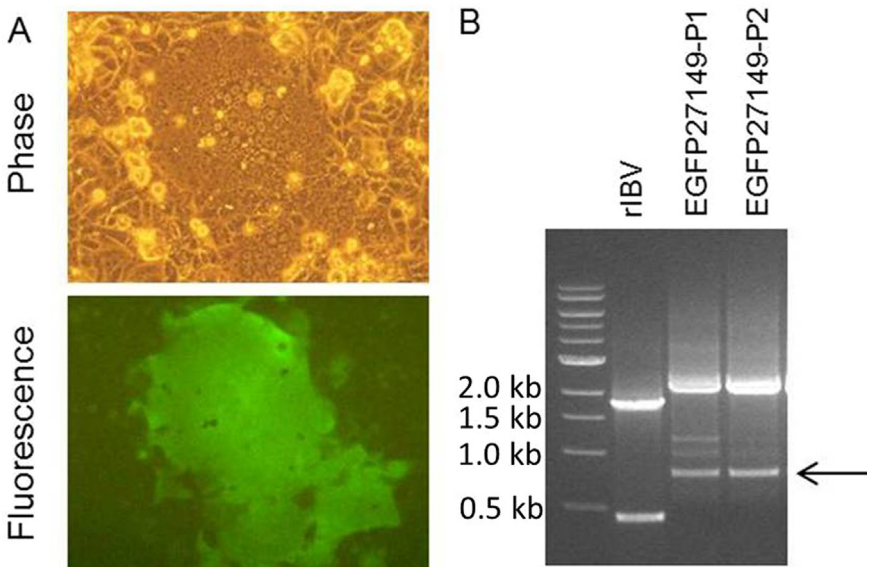


**Fig. 3.** Insertion of EGFP ORF between 27149 and 27150 nt in IBV genome allows the recovery of recombinant virus IBV-EGFP27149 and EGFP expression in virus-infected Vero cells. A. The phase-contrast and fluorescence images of cells infected with passage 2 of IBV-EGFP27149 indicated the expression of EGFP. B. RT-PCR detected the presence of EGFP ORF in subgenomic RNA (indicated in arrow).

**Table 1**
Core sequences in leader and body TRS.

| Location | Core sequences in leader and body TRS |
|---|---|
| Leader | UUAACUUAACAA**AACGG**ACTT |
| S | AAAACUGAACAAAAGACAGAC |
| 3a/3b | GUAACUGAACAAUACAGACCU |
| M | AAAACUUAACAAUCCGGAAUU |
| 5a/5b | AAAACUUAACAAAUACGGACG |
| N | CUUUCUUAACAAAGCAGGACA |
| ncRNA | –UGAGUAACAU**AAUGG**ACCU |

nucleotides (A27105/A27106/C27107) are involved in the effective ncRNA generation. The results confirmed previous report that IBV can synthesize sgRNA via template switch mediated by a noncanonical core sequence (Bentley et al., 2013) Notably, the mutant virus carrying four mutations (A27100U/A27111U/G27113C/G27114C) was also unable to produce ncRNA (Fig. 4), suggesting these nucleotides are required for ncRNA production. Because the sequence motif (A27100/A27111/G27113/G27114) located downstream of the truncated CS (UAACA) also exists downstream of the CS (CUUAACAA) in the leader TRS (Table 1, marked in bold), our result prove that the sequences downstream of the CS exert a stronger influence on coronavirus sgRNA synthesis (Sola et al., 2005). Taken together, the results confirm that the ncRNA generation involves a discontinuous transcription process in which the 5′ leader sequence and 3′-UTR are fused through the transcription-regulating sequences in the 3′ end of the leader and in the 5′ end of the 3′-UTR.

### *3.3. ncRNA has little effect on viral RNA synthesis and virus phenotype in Vero cells*

The mutant virus C27107G was selected for further experiments because it is not capable of producing ncRNA and carries only one nucleotide change, compared to rIBV. Plaque assay on Vero cells showed both viruses did not display major differences in plaque morphology and in virus growth properties (Fig. 5A). Moreover, real-time RT-PCR and Western blot were performed to analyze the expression of S and N genes at different time points post-infection, respectively. Similarly, no significant differences were detected at both RNA level and protein level (Fig. 5B, C). The results suggest that ncRNA has little effects on viral replication and viral cytopathicity in Vero cells.

## 4. Discussion

In this report, we have identified an ncRNA in IBV-infected cells and revealed that this ncRNA is generated via discontinuous transcription mechanism by reverse genetics and mutagenesis for the first time. Although the ncRNA has no or little effect on viral replication and pathogenesis in Vero cells, roles in IBV pathogenesis in chicken and virus-host interplay are unknown, needing to further study.

Coronaviruses employ a discontinuous transcription mechanism to synthesize subgenomic mRNAs through template switch taking place in the transcription-regulating sequences in the 3′ end of the leader (TRS-L) and in the intergenic region preceding each mRNA body (TRS-B) during negative RNA synthesis (Baric and Yount, 2000; Zúñiga et al., 2004; Masters, 2006; Sawicki et al., 2007). The five sgRNAs (mRNAs 2–6) of IBV, which are readily detected by Northern blotting, possess the canonical core sequence (5′- CU(U/G)AACAA-3′) (Table 1). It has been reported that coronaviruses, such as severe acute respiratory syndrome coronavirus, mouse hepatitis virus and IBV, can use non-canonical CS to synthesize sgRNA via discontinuous transcription mechanism (Zhang and Liu, 2000; Hussain et al., 2005; Bentley et al., 2013). In this report, we have identified the existence of a novel sgRNA derived mainly from the 3′ UTR of IBV in the IBV-infected cells (Fig. 1). The synthesis of this sgRNA is mediated by a truncated CS ($_{27104}$UAACA$_{27108}$) identical to nucleotides of 3–7 of IBV CS. Among which at least three nucleotides (A27105/A27106/C27107) are involved in the effective sgRNA generation (Figs. 2 and 4), providing more evidence for the use of noncanonical transcriptional signals in synthesis of coronavirus sgRNAs. In addition, we verified that the sequence motif (A27100/A27111/G27113/G27114) located downstream of the truncated CS (UAACA) is necessary for ncRNA generation (Fig. 4), reinforcing the importance of nucleotides immediately flanking CS in coronavirus sgRNA synthesis (Sola et al., 2005).

Interestingly, when BLAST search in GenBank, we find that the sequence motif (UAACA) is conserved at 5′ end of 3′ UTR of IBV strain Beaudette and its derivants, Arkansas DP1, and turkey coronavirus but not for strain M41, H120, H52, A2, and several field isolates in China. Therefore, whether these viruses can produce ncRNA and how ncRNA affects the viral pathogenecity remain to be determined.

## Acknowledgments

This work was financially supported by grants from the National Natural Science Foundation of China (No. 31572490) and the Department of Science and Technology, Hubei Provincial People's Government, China (No. 2013BHE020)

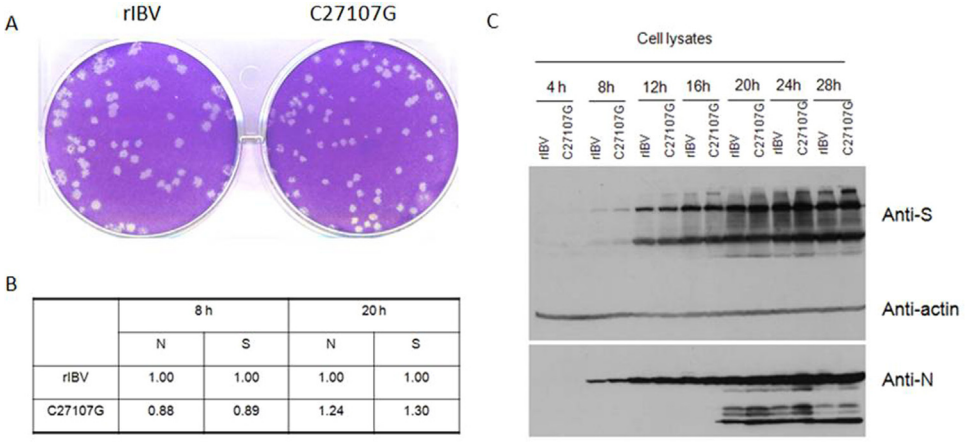


| | 8 h | | 20 h | |
|---|---|---|---|---|
| | N | S | N | S |
| rIBV | 1.00 | 1.00 | 1.00 | 1.00 |
| C27107G | 0.88 | 0.89 | 1.24 | 1.30 |

**Fig. 5.** Effect of ncRNA on plaque morphology and viral replication. A. Plaque assay. Vero cells in 6-well plates were infected with a dilution series of rIBV and mutant virus IBV-C27107G for 1 h, respectively. After washing twice with medium, cells were overlaid with 0.4% agar in FBS-free DMEM, incubated at 37 °C for 3–4 days, fixed with 10% formaldehyde, and stained with 0.2% crystal violet. B. Quantitative analysis of sgRNA synthesis of N and S. Total RNA (2 μg) extracted from the Vero cells infected with rIBV and IBV-C27107G at an MOI of 0.5 PFU/cell at 8 and 20 h post-infection was used for reverse transcription using primer oligo(dT)18 respectively. Amplification and data collection were performed as manufacturer's instruction (Applied Biosystems 7500 real-time PCR system). The relative gene expression levels were measured using GAPDH as an internal reference, and normalized to gene expression in mock-infected cells (relative expression = 1). All experiments were performed in triplicate. C. Western blotting. Vero cells were infected with rIBV and IBV-C27107G at an MOI of 0.5 PFU/cell at the indicated time point. Cell lysates from the indicated time point were prepared for Western blotting using antibody against S or N protein.

## References


Akiyama, B.M., Laurence, H.M., Massey, A.R., Costantino, D.A., Xie, X., Yang, Y., Shi, P.Y., Nix, J.C., Beckham, J.D., Kieft, J.S., 2016. Zika virus produces noncoding RNAs using a multi-pseudoknot structure that confounds a cellular exonuclease. Science 354, 1148–1152.

Albrecht, J.C., Fleckenstein, B., 1992. Nucleotide sequence of HSUR 6 and HSUR 7, two small RNAs of herpesvirus saimiri. Nucleic Acids Res 20, 1810.

Arvey, A., Tempera, I., Tsai, K., Chen, H.S., Tikhmyanova, N., Klichinsky, M., Leslie, C., Lieberman, P.M., 2012. An atlas of the Epstein-Barr virus transcriptome and epigenome reveals host-virus regulatory interactions. Cell Host Microbe 12, 233–245.

Baric, R.S., Yount, B., 2000. Subgenomic negative-strand RNA function during mouse hepatitis virus infection. J. Virol. 74, 4039–4046.

Bentley, K., Keep, S.M., Armesto, M., Britton, P., 2013. Identification of a noncanonically transcribed subgenomic mRNA of infectious bronchitis virus and other gammacoronaviruses. J. Virol. 87, 2128–2136.

Bidet, K., Dadlani, D., Garcia-Blanco, M.A., 2014. G3BP1 G3BP2 and CAPRIN1 are required for translation of interferon stimulated mRNAs and are targeted by a dengue virus non-coding RNA. PLoS Pathog. 10, e1004242.

Bloom, D.C., 2004. HSV LAT and neuronal survival. Int Rev. Immunol. 23, 187–198.

Bogerd, H.P., Karnowski, H.W., Cai, X., Shin, J., Pohlers, M., Cullen, B.R., 2010. A mammalian herpesvirus uses noncanonical expression and processing mechanisms to generate viral MicroRNAs. Mol. Cell 37, 135–142.

Borah, S., Darricarrere, N., Darnell, A., Myoung, J., Steitz, J.A., 2011. A viral nuclear noncoding RNA binds re-localized poly(A) binding protein and is required for late KSHV gene expression. PLoS Pathog. 7, e1002300.

Bowden, R.J., Simas, J.P., Davis, A.J., Efstathiou, S., 1997. Murine gammaherpesvirus 68 encodes tRNA-like sequences which are expressed during latency. J. Gen. Virol. 78, 1675–1687.

Campbell, C.L., Keene, K.M., Brackney, D.E., Olson, K.E., Blair, C.D., Wilusz, J., Foy, B.D., 2008. Aedes aegypti uses RNA interference in defense against Sindbis virus infection. BMC Microbiol 8, 47.

Cavanagh, D., 2005. Coronaviruses in poultry and other birds. Avian Pathol. 34, 439–448.

Cazalla, D., Yario, T., Steitz, J.A., 2010. Down-regulation of a host microRNA by a Herpesvirus saimiri noncoding RNA. Science 328, 1563–1566.

Diebel, K.W., Smith, A.L., van Dyk, L.F., 2010. Mature and functional viral miRNAs transcribed from novel RNA polymerase III promoters. RNA 16, 170–185.

Ensser, A., Fleckenstein, B., 2005. T-cell transformation and oncogenesis by gamma2-herpesviruses. Adv. Cancer Res. 93, 91–128.

Fang, S., Chen, B., Tay, F.P., Ng, B.S., Liu, D.X., 2007. An arginine-to-proline mutation in a domain with undefined functions within the helicase protein (Nsp13) is lethal to the coronavirus infectious bronchitis virus in cultured cells. Virology 358, 136–147.

Hussain, S., Pan, J., Chen, Y., Yang, Y., Xu, J., Peng, Y., Wu, Y., Li, Z., Zhu, Y., Tien, P., Guo, D., 2005. Identification of novel subgenomic RNAs and noncanonical transcription initiation signals of severe acute respiratory syndrome coronavirus. J. Virol. 79, 5288–5295.

Kincaid, R.P., Burke, J.M., Sullivan, C.S., 2012. RNA virus microRNA that mimics a B-cell oncomiR. Proc. Natl. Acad. Sci. USA 109, 3077–3082.

Kulesza, C.A., Shenk, T., 2004. Human cytomegalovirus 5-kilobase immediate-early RNA is a stable intron. J. Virol. 78, 13182–13189.

Kulesza, C.A., Shenk, T., 2006. Murine cytomegalovirus encodes a stable intron that facilitates persistent replication in the mouse. Proc. Natl. Acad. Sci. USA 103, 18302–18307.

Lee, N., Moss, W.N., Yario, T.A., Steitz, J.A., 2015. An EBV noncoding RNA base pairs with nascent RNA to enable PAX5 transcription factor binding to viral DNA. Cell 160, 607–618.

Masters, P.S., 2006. The molecular biology of coronaviruses. Adv. Virus Res. 66, 193–292.

Mathews, M.B., Shenk, T., 1991. Adenovirus virus-associated RNA and translation control. J. Virol. 65, 5657–5662.

Miller, W.A., Shen, R., Staplin, W., Kanodia, P., 2016a. Noncoding RNAs of plant viruses and viroids: sponges of host translation and RNA interference machinery. Mol. Plant Microbe Interact. 29, 156–164.

Miller, W.A., Shen, R., Staplin, W., Kanodia, P., 2016b. Noncoding RNAs of plant viruses and viroids: sponges of host translation and RNA interference machinery. Mol. Plant Microbe Interact. 29, 156–164.

Moon, S.L., Anderson, J.R., Kumagai, Y., Wilusz, C.J., Akira, S., Khromykh, A.A., Wilusz, J., 2012. A noncoding RNA produced by arthropod-borne flaviviruses inhibits the cellular exoribonuclease XRN1 and alters host mRNA stability. RNA 18, 2029–2040.

Pijlman, G.P., Funk, A., Kondratieva, N., Leung, J., Torres, S., van der Aa, L., Liu, W.J., Palmenberg, A.C., Shi, P.Y., Hall, R.A., Khromykh, A.A., 2008. A highly structured, nuclease-resistant, noncoding RNA produced by flaviviruses is required for pathogenicity. Cell Host Microbe 4, 579–591.

Reich, P.R., Forget, B.G., Weissman, S.M., 1966. RNA of low molecular weight in KB cells infected with adenovirus type 2. J. Mol. Biol. 17, 428–439.

Sawicki, S.G., Sawicki, D.L., Siddell, S.G., 2007. A contemporary view of coronavirus transcription. J. Virol. 81, 20–29.

Schnettler, E., Sterken, M.G., Leung, J.Y., Metz, S.W., Geertsema, C., Goldbach, R.W., Vlak, J.M., Kohl, A., Khromykh, A.A., Pijlman, G.P., 2012. Noncoding flavivirus RNA displays RNA interference suppressor activity in insect and Mammalian cells. J. Virol. 86, 13486–13500.

Schuessler, A., Funk, A., Lazear, H.M., Cooper, D.A., Torres, S., Daffis, S., Jha, B.K., Kumagai, Y., Takeuchi, O., Hertzog, P., et al., 2012. West Nile virus noncoding subgenomic RNA contributes to viral evasion of the type I interferon-mediated antiviral response. J. Virol. 86, 5708–5718.

Shen, H., Fang, S.G., Chen, B., Chen, G., Tay, F.P., Liu, D.X., 2009. Towards construction of viral vectors based on avian coronavirus infectious bronchitis virus for gene delivery and vaccine development. J. Virol. Methods 160, 48–56.

Skalsky, R.L., Cullen, B.R., 2015. EBV noncoding RNAs. Curr. Top. Microbiol Immunol. 391, 181–217.

Sola, I., Moreno, J.L., Zúñiga, S., Alonso, S., Enjuanes, L., 2005. Role of nucleotides immediately flanking the transcription-regulating sequence core in coronavirus subgenomic mRNA synthesis. J. Virol. 79, 2506–2516.

Steitz, J., Borah, S., Cazalla, D., Fok, V., Lytle, R., Mitton-Fry, R., Riley, K., Samji, T., 2010. Noncoding RNPs of viral origin. Cold Spring Harb. Perspect. Biol. 165–179.

Stern-Ginossar, N., Weisburd, B., Michalski, A., Le, V.T., Hein, M.Y., Huang, S.X., Ma, M., Shen, B., Qian, S.B., Hengel, H., et al., 2012. Decoding human cytomegalovirus. Science 338, 1088–1093.

Sun, R., Lin, S.F., Gradoville, L., Miller, G., 1996. Polyadenylylated nuclear RNA encoded by Kaposi sarcoma-associated herpesvirus. Proc. Natl. Acad. Sci. USA 93, 11883–11888.

Wang, Z., Shen, W., Cheng, F., Deng, X., Engelhardt, J.F., Yan, Z., Qiu, J., 2017. Parvovirus expresses a small noncoding RNA that plays an essential role in virus replication. J. Virol. 191 (e02375-16).

Wilson, J.L., Vachon, V.K., Sunita, S., Schwartz, S.L., Conn, G.L., 2014. Dissection of the adenoviral VA RNAI central domain structure reveals minimum requirements for RNA mediated inhibition of PKR. J. Biol. Chem. 289, 23233–23245.

Zhang, X., Liu, R., 2000. Identification of a noncanonical signal for transcription of a novel subgenomic mRNA of mouse hepatitis virus: implication for the mechanism of coronavirus RNA transcription. Virology 278, 75–85.

Zhong, W., Ganem, D., 1997. Characterization of ribonucleoprotein complexes containing an abundant polyadenylated nuclear RNA encoded by Kaposi's sarcoma-associated herpesvirus (human herpesvirus 8). J. Virol. 71, 1207–1212.

Zúñiga, S., Sola, I., Alonso, S., Enjuanes, L., 2004. Sequence motifs involved in the regulation of discontinuous coronavirus subgenomic RNA synthesis. J. Virol. 78, 980–994.